WARSAW UNIVERSITY OF TECHNOLOGY Index 351733
FACULTY OF CIVIL ENGINEERING
COMMITTEE FOR CIVIL AND WATER ENGINEERING
POLISH ACADEMY OF SCIENCES ISSN 1230-2945

DOI: 10.24425/ace.2022.140167

ARCHIVES OF CIVIL ENGINEERING

Vol. LXVIII ISSUE 1 2022

 pp. 255 – 274

Research paper

Adaptation of the total stiffness method to the load distribution of stiffening masonry walls according to Eurocode 6

Radosław Jasiński[1], Krzysztof Grzyb[2]

Abstract: The internal forces in stiffening walls are usually determining by numerical methods. Extreme values of forces and displacements can be achieved without significant problems. The numerical model is always labour-intensive; therefore, it is not used for single-family or multi-family buildings with a simple wall layout. To calculate efficiently internal forces in such walls uses an analytical model. Eurocode 6 (prEN 1996-1-1: 2019) does not provide specific guidelines for determining geometrical characteristics and procedures for calculating the values of internal forces in the stiffening walls. The use of numerical methods and other reliable methods was allowed. The paper presents the adaptation of the total stiffness method to determine internal forces in a building with a simple wall system. The method was based on dividing the masonry wall with openings into pillars, lintels, bottom sprandels and flanged walls. The analytical results were compared with linear-elastic FEM calculations. It has been demonstrated that flexural stiffness, shear stiffness and localization of rotation centre (RC) had a crucial impact on masonry structure.

Keywords: masonry structures, stiffening walls, load distribution, rotation centre

[1]DSc., PhD., Eng., Silesian University of Technology, Faculty of Civil Engineering, ul. Akademicka 5, 44-100 Gliwice, Poland, e-mail: radoslaw.jasinski@polsl.pl, ORCID: 0000-0003-4015-4971
[2]MSc., Eng., Silesian University of Technology, Faculty of Civil Engineering, ul. Akademicka 5, 44-100 Gliwice, Poland, e-mail: krzysztof.grzyb@polsl.pl, ORCID: 0000-0001-9039-5015

1. Introduction

According to Eurocode 6 [1] (subsection 3.9.12), a stiffening wall is each wall intended to absorb horizontal forces acting in a plane, ensuring the geometric stability of the building and limiting the horizontal displacement of structural elements. An adequately designed arrangement of stiffening walls should eliminate horizontal displacements – thanks to which the calculating of load-bearing walls, inter-hole pillars or columns can be performed without the influence of eccentricities caused by horizontal loads. All structural walls are stiffening walls, while the other walls can be stiffening walls, provided that the building structure allows for transferring external horizontal loads [2], and the thickness ($t_{ef} \geq 180$ mm) meets the design requirements of the standard [1]. The horizontal loads acting on the stiffening walls may also occur together with vertical load derived from the self-weight of the structure and live loads. The vertical loads depend on whether the stiffening wall is also a load-bearing wall and how it is located in the building. Historically, in masonry buildings – in which the structural walls were characterized by large thickness – the computational verification of the spatial stiffness was usually unnecessary. The load-bearing walls perfectly acted as stiffening walls, minimizing horizontal displacements.

Currently, there is a tendency to reduce the thickness of the walls and use thin-layer joints, longitudinal strip joints or unfitted head joints – which significantly reduces the stiffness of each wall. Therefore, the wall should be designed for compression and shearing – which is related to the calculations of internal forces. A universal tool that enables determining loads and displacements is numerical calculations using the Finite Element Method (FEM). The FEM model is justified in calculating multi-storey buildings with complex structures, for which analytical methods are inappropriate. For single-family or multi-family buildings with a simple wall system – which in most cases include masonry structures – the use of FEM does not seem reasonable. In such cases, an analytical method provides a safe and quick estimation of internal forces.

The main goal of this study was adaptation the method of total stiffness to the distribution of loads on the stiffening walls in a building with a simple wall system – according to the recommendations of Eurocode 6. The introduction presents the standard rules for stiffening walls placed in Eurocode 6. Then, a more detailed calculation procedure was proposed. The presented calculations method was compared with FEM calculations for a building model with a simple wall system.

2. Stiffening walls calculation in standard regulations

In the national regulations before preceding the unification of design procedures with European regulations [3–5], there was no information on stiffening wall calculation in masonry structures. The standards are supplemented by the national guidelines for the design of masonry buildings [6], consisting of guidelines provided in German standards DIN 1053 [7] and international recommendations of the CIB [8]. The work contains detailed guidelines for stiffening masonry walls calculations, developed analogously to buildings erected with industrialized methods. Tie beams (ring beams) and reinforced concrete slabs realized the bracing of the masonry walls. The criterion of taking over the wind load was the flexural stiffness and shear stiffness. The openings in the walls were taken into account by introducing the equivalent wall stiffness calculated on the reduction factor η_A – developed on a coupled-wall model [9]. This method – due to the omission of connection the stiffening walls with perpendicular walls in taking over the loads and lowering the lintel stiffness – led to the determination of the maximum edge stress forces even with a 30% excess of the exact calculations. In Polish regulations PN-B-03002:1999 [10] and PN-B-03002:2007 [5] recommendations have been more detailed and harmonized with ENV 1996-1-1: 1994 [11] and PN-EN 1996-1-1:2010 [12]. The stiffening walls were divided due to the horizontal (wind) load and the stiffening walls due to the vertical displacements of the subsoil (uneven settlement). The arrangements included in [6] were adopted to design stiffening walls due to the horizontal loads.

In addition to the ULS conditions – an additional SLS deformation condition was introduced, which became the primary condition for checking the stiffening walls due to vertical displacements of the subsoil. Other European standards preceding the Eurocode era: British [13], Irish [14], German [15, 16], Swiss [17, 18] Norwegian, [19] and Russian [20] were limited only to the information that the forces in the stiffening walls should be calculated in proportion to their bending stiffness, using linear-elastic material models. No information is given on the influence of the torsion of the building and other design conditions regarding the effect of openings. The regulations and guidelines in the NBCC 2005 recommendations (National Building Canadian Code) [21] are much more detailed and valuable (from a practical approach). According to these regulations, the horizontal loads acting on the building consists of the location of the gravity centre (GC) walls layout (seismic influences), the centre of the resultant external load LC (wind load), and then calculating the location of the rotation centre (RC). The distribution of loads on the stiffening walls assumes that the slabs are treated as non-deformable shell in their plane. The calculation procedure of internal forces in walls is similar to those proposed in Polish regulations [6]. The difference is in the calculation of the wall stiffness. The cantilever model is not being used, but the division of the wall into its components (a cantilever or double-fixed static scheme of each wall component is assumed). A limitation of the standard is adjusting the procedure only to stiffening walls with window openings.

The American standard [22] – in the field of stiffening walls – provides very perfunctory information that the distribution of horizontal loads to each stiffening element depends on the stiffness of the walls and the stiffness of the slabs. In calculation wall stiffness, the following walls are distinguished: squat ($h/l < 0.25$), rectangular ($0.25 < h/l < 4.0$) and slender ($h/l > 4.0$). The horizontal loads acting on the building can take over the stiffening walls parallel to the load direction. Therefore, the walls along the length and width of the building should be analyzed separately. The method of determining loads on walls was not given. However, it was stated that generally accepted methods of calculating forces in walls should be used. The coupled-wall cantilever method was allowed to be used in walls with horizontal connectors made as masonry lintels. The American Masonry

Structural Design for Buildings [23] guidelines are slightly more detailed than the previous one. The distribution of horizontal loads in a multi-storey masonry building depends on the proportion of the slabs' stiffness and walls parallel to the direction of the external load. The stiffnesses of the stiffening walls on each storey were inversely proportional to their total displacement, which consisted of bending and shear displacements. In determining the wall's stiffness, the integrated stiffening system was divided into individual stiffening groups. Generally, the separation of the system was taken in places where walls connect or intersect. The division method influenced the overall structure stiffness, similar to the openings and connections with perpendicular walls. The regulations explicitly recommend that the effect of openings in the stiffening walls be taken into account. The analysis of walls with openings depended on the relative stiffness of the vertical pillars between the openings, lintels and the building's geometry. Chinese regulations GB 50003-2001: 2001 [24] assumed a frame model of the building with linear-elastic material in calculation models. At each floor level, virtual supports were introduced to represent internal stiffening elements. Internal forces arose in the bars and were induced by loads occurring in all the stiffening walls on the storeys. The distribution of loads on walls was based on the assumption that all walls had the same geometry, and the impact of building torsion was not significant.

3. Eurocode 6 regulations

The calculation rules of the stiffening walls in chapter 7.5.5 of Eurocode 6 [1], similarly to most of the standard regulations presented in section two – are pretty laconic. The standard arrangements are limited to a calculation based on the linear-elastic material model – taking into account the wall's openings. It can be assumed that the calculation model of a stiffening wall or a wall with an opening is a rectangular plane model. The possibility of taking over external loads by stiffening walls and adjacent parts of walls should be enclosed in calculations. The transverse wall fragment length that takes over external loads together with stiffening wall depends on various factors. By Eurocode, the following length depends on stiffening wall thickness (t), height (h_{tot}) and distance between

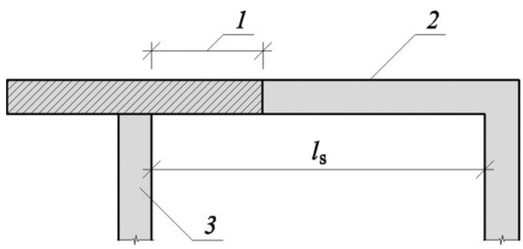

Fig. 1. The length of the transverse wall fragment, which can be assumed as the stiffening wall: 1 – a fragment of a transverse wall contributing with a stiffening wall of length $b_{\text{eff}1}$, 2 – transverse wall, 3 – stiffening wall

other stiffening walls (l_s) and opening height h. The above relationships are expressed in (3.1) and shown in Figure 1.

$$b_{\text{eff1}} = \min \begin{cases} h_{\text{tot}}/5 \\ l_{\text{s}}/2 \\ h/2 \\ 8 \cdot t \end{cases} \tag{3.1}$$

If the walls perpendicular to the stiffening wall have window or door openings with dimensions smaller than $h/4$ or $l/4$ (h, l – height and length of the transverse wall), the transverse wall can be treated as a wall without openings. When openings are larger than $h/4$ or $l/4$, they should be treated as the ends of the transverse wall. The omission of smaller openings has a positive effect as it increases the stiffness of the stiffening group. However, the presence of additional wall sections can complicate the calculations. In buildings with slabs treated as a rigid plane, i.e. with monolithic reinforced concrete slabs supported on the walls through tie beams – the horizontal load can be distributed proportionally to the flexural stiffness of each wall. Therefore, it is assumed that all walls parallel to the external load are stiffening walls, and the displacements of their edges within one story are identical. Another situation occurs when the building has a slab that cannot be treated as the rigid plane in both directions. In this case, the standard mentions prefabricated slabs, but this group also includes rib-and-block slabs or light wooden slabs.

In conclusion, according to those presented code regulations and the provisions of Eurocode 6, there are no specific regulations that enable a practical design of stiffening walls. No fundamental provisions cover detailed guidelines for determining geometric characteristics and the distribution of internal forces in the stiffening walls. In all regulations, the critical issue is determining the wall stiffness, which is the criterion for distributing external loads.

4. Proposal of stiffening walls calculation method

Within designing the building's structural system, one should aim for a symmetrical arrangement of the stiffening walls. Then the distribution of loads on particular walls in each direction will be similar, and the building's spatial stiffness will be the highest. However, when the building's layout is irregular, there are one-directional slabs or arrangement of load-bearing walls forced by functional reasons not be symmetrical – horizontal loads may cause additional torsion of the building and increase the displacement of the walls.

The standard [1] clearly states that if the coordinates of the point of load centre (LC) are different from the rotation centre (RC) coordinates, then the torsion effect should be taken into account. However, no details are given on determining the stiffness centre and considering the torsion effect – leaving freedom in the calculation method. The Eurocode's simplification assumes that loads can only be taken by walls located parallel to the external load. The distribution of loads proportional to the wall's stiffness can only occur when there are rigid slabs. Such an assumption causes the integrated structure to be divided into unconnected stiffening units or stiffening walls with fragments of transverse walls treated as one stiffening section (flanged walls). Determining the rotation centre (RC) location consists of dividing the structure into single, not connected wall fragments in the direction of the length and width of the building [2, 25]. Then, for each wall, the stiffnesses K_{xi} and K_{yi} are calculated. The distances a_{xi}, a_{yi} between their stiffening centres and the load centre (LC) are determined. The coordinates of the rotation centre (RC) are derived from the equilibrium of forces according to the following formulas:

$$x_R = \frac{\sum_i (a_{xi}K_{xi})}{\sum_i K_{xi}}, \qquad y_R = \frac{\sum_i (a_{yi}K_{yi})}{\sum_i K_{yi}} \tag{4.1}$$

in which: a_{xi}, a_{yi} – the distance between the load centre (LC) and the rotation centres of the particular wall or stiffening group, K_{xi}, K_{yi} – stiffness of the wall or stiffening group.

In calculation – the position of the building's stiffening centre – it is assumed that the walls along the length and in the width direction are not connected. Therefore the rotation centre of each wall band is the same as the gravity centre. At this stage, a preliminary assessment is made of the correctness of the building's stiffening system. Bases on the building's rotation centre location, it is possible to calculate internal forces in the stiffening group. Within selecting the stiffening group, all wall fragments or wall strips that will not determine the building's spatial stiffness may be omitted. Slender pillars between the windows, single masonry columns, infilling walls or wall fragments connected with stiffening walls by connectors can be ignored. The horizontal forces H_x and H_y acting the building in the middle of the tie-beams cause torsion moment $M_{sx} = H_x x_R$ and $M_{sy} = H_y y_R$. The transverse forces in each stiffening group on any storey are the sum of the transverse forces caused by the action of external forces H_x or H_y and the torsional moments M_{sx} and M_{sy} calculated from the following relationships [9]:

– shear forces induced by the load H_x and H_y:

$$H_{x,i} = H_x \frac{K_{y,i}}{\sum_i K_{y,i}}, \qquad H_{y,i} = H_y \frac{K_{x,i}}{\sum_i K_{x,i}} \tag{4.2}$$

– shear forces induced by torsional moments M_{sx} and M_{sy}:

$$\begin{aligned} H_{xs,i} &= \pm M_{sx} \frac{\bar{a}_{xi}K_{y,i}}{\sum_i \bar{a}^2_{xi}K_{x,i} + \sum_i \bar{a}^2_{yi}K_{y,i}}, \qquad H_{ys,i} = \pm M_{sx} \frac{\bar{a}_{xi}K_{y,i}}{\sum_i \bar{a}^2_{xi}K_{x,i} + \sum_i \bar{a}^2_{yi}K_{y,i}} \\ H_{xs,i} &= \pm M_{sy} \frac{\bar{a}_{xi}K_{y,i}}{\sum_i \bar{a}^2_{xi}K_{x,i} + \sum_i \bar{a}^2_{yi}K_{y,i}}, \qquad H_{ys,i} = \pm M_{sy} \frac{\bar{a}_{xi}K_{y,i}}{\sum_i \bar{a}^2_{xi}K_{x,i} + \sum_i \bar{a}^2_{yi}K_{y,i}} \end{aligned} \tag{4.3}$$

The bending moments are following:

– bending moments caused by load H_x and H_y:

$$M_{ox,i} = M_{ox}\frac{K_{x,i}}{\sum\limits_i K_{x,i}}, \qquad M_{oy,i} = M_{ox}\frac{K_{y,i}}{\sum\limits_i K_{y,i}} \tag{4.4}$$

– bending moments due to torsional moments of the building M_{sx} and M_{sy}:

$$M_{sx,i} = \pm H_{xs,i}h_m, \qquad M_{sy,i} = \pm H_{ys,i}h_m \tag{4.5}$$

where: $\bar{a}_{xi}$, $\bar{a}_{yi}$ – distances of the gravity centre of the wall bands to the rotation centre (RC), h_m – wall height.

A single wall divided into zones weakened by openings and zones of greater stiffness (lintels and bottom sprandel) to determine the wall's stiffness – Fig. 2. The displacement from a unit load of the upper edge of the wall was generated by a concentrated force and a bending moment, analogically to the Canadian regulations [21]. Through concentrated force and bending moment generated the unit displacement of the upper edge of the wall, analogically to the Canadian regulations [21]. The total displacement of the upper edge of the wall is the sum of the displacements of the bottom sprandels, inter-opening pillars and lintels and is calculated from the relationship:

$$\Delta_w = {}^{\mathrm{A}}\Delta_w + {}^{\mathrm{P}}\Delta_w + {}^{\mathrm{B}}\Delta_w \tag{4.6}$$

in which: ${}^{\mathrm{A}}\Delta_w$, ${}^{\mathrm{B}}\Delta_w$ – displacement of the bottom sprandel and lintel, ${}^{\mathrm{P}}\Delta_w$ – displacement of the wall with the opening of height h_0 and length l.

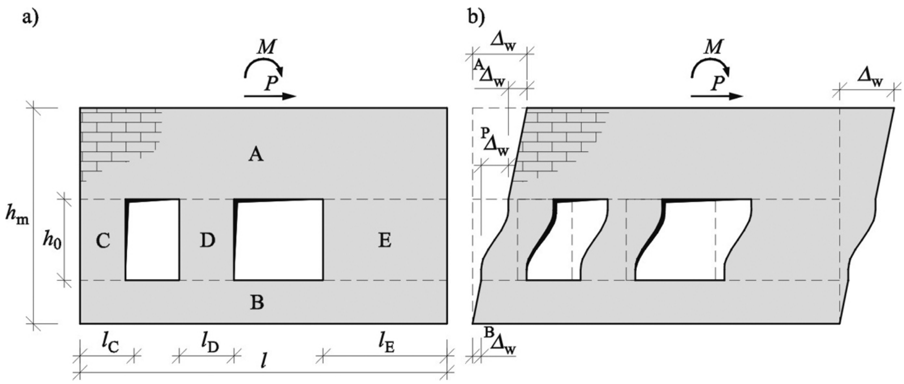

Fig. 2. Total wall stiffness method: a) division of the wall with openings into component elements, b) wall deformations caused by horizontal loads

The displacements of the wall components are determined depending on the geometry and boundary conditions of the wall. If the ratio of the height to the length of the wall is $h/l > 2$, the effects of tangential stresses in determining the wall stiffness can be neglected.

Otherwise, the stiffness should be determined, taking into account shear deformations. The stiffnesses of the walls fixed in different ways with different dimensions loaded with a concentrated force are given in Table 1.

Table 1. Stiffness of walls subjected to shear with bending [26–28]

Static scheme of the wall	$h/l \le 2$		$h/l \ge 2$	
	Force P	Moment M	Force P	Moment M
Cantilever type "C"	$K_P = \dfrac{1}{\dfrac{h_m^3}{3EI} + \dfrac{1,2h_m}{GA}}$ 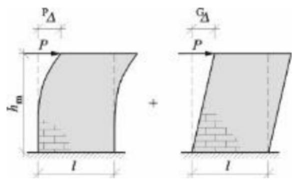	$K_M = \dfrac{2EI}{h_m^2}$ 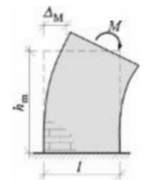	$K_M = \dfrac{3EI}{h_m^3}$ 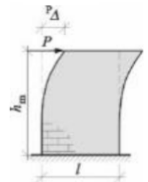	$K_M = \dfrac{2EI}{h_m^2}$ 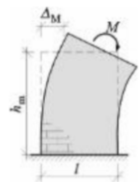
Double-fixed type "F"	$K_P = \dfrac{1}{\dfrac{h_m^3}{12EI} + \dfrac{1,2h_m}{GA}}$ 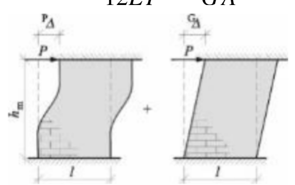	–	$K_M = \dfrac{12EI}{h_m^3}$ 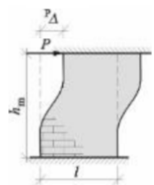	–

After determining the total displacement of the wall, its stiffness is calculated from the relationship:

$$K_w = \frac{1}{\Delta_w} \tag{4.7}$$

Δ_w – is the total displacement of the top edge of the wall induced by unit load $P = 1$.

5. The example of internal forces calculations in stiffening walls

The subject of the calculations was a model of a single-story building made of autoclaved aerated concrete masonry units with a modulus of elasticity equal to E_m = 2041 N/mm^2, a shear modulus of G_m = 475 N/mm^2 and a Poisson ratio of ν_m = 0.18 [29–31].

The layout of the building had a square shape with dimensions $B = L = 4.0$ m and wall thicknesses $t_1 = t_2 = t_A = t_B = 0.18$ m. The $h_m = 2.4$ m high walls were finished with a reinforced concrete beam$h_w = 0.22$ m height. A reinforced concrete slab with a thickness of $h_s = 0.16$ m was supported on the tie-beam. In the analytical method, one geometric solution and two load variants were assumed. In the variant marked as I, the load with the H_X force acted parallel to the X-axis, and in case II, the load with the H_Y force acted parallel to the Y-axis. A door opening with a width of ${}^{A}l_0 = 1.0$ m and height $h_0 = 1.92$ m was made in the wall along the A-axis. The lengths of the pillars were identical, equal to ${}^{A}l_C ={}^{A} l_D = 1.32$ m. A window opening with a width of ${}^{1}l_0 = 1.0$ m and height of $h_0 = 1.0$ m was made in the wall along axis 1. In this wall, the lengths of the inter-hole pillars were identical and amounted to ${}^{1}l_C ={}^{1} l_D = 1.32$ m. Loads were assumed as concentrated forces in cases I and II were respectively $H_x = -1.0$ kN and $H_y = -1.0$ kN. The model geometries and the values of internal forces acting on the walls are shown in Fig. 3. The model was solved using two possible static schemes of inter-hole pillars – double-fixed type "F" and cantilever type "C".

The analytical calculations of the stiffening walls were carried out according to the following procedure:

a) the lengths of b_{eff1} walls have been determined by the recommendations of Eurocode 6 [1] according to formula (3.1),

b) walls with openings were divided into component elements, as shown in Fig. 2. Moments of inertia of the component elements were calculated, taking into account the flanged walls,

c) two static schemes were assumed: "C" – cantilever wall, "F" – double-fixed wall,

d) the stiffnesses K of the wall components were determined according to the formulas in Table 1,

e) the stiffness of stiffening walls was determined according to Fig. 2 and relationship (4.6),

f) the distances of the rotation centres of = walls a_{xi}, a_{yi} in relation to the load centre were determined (LC),

g) the position of the rotation centre (RC) was calculated according to the formula (4.1),

h) internal forces in stiffening walls were calculated according to formulas (4.2)–(4.5). The results of the geometric data and wall stiffness calculations are given in Table 2. Stiffnesses with the changed static scheme of the inter-hole pillars are given in brackets.

Based on the formula (3.1), the coordinates of the building's rotation centre location were determined: $x_R = 0.10$ m, $y_R = -0.32$ m. On the other hand, using static cantilever schemes of inter-hole pillars, coordinates of the rotation centre were obtained: $x_R = 0.16$ m, $y_R = -0.61$ m. Based on formulas (4.1)–(4.4), the values of internal forces in walls were calculated. The calculation's results according to the analytical model are summarized in Table 3. The results are presented for the cantilever model and the double-fixed static schemes.

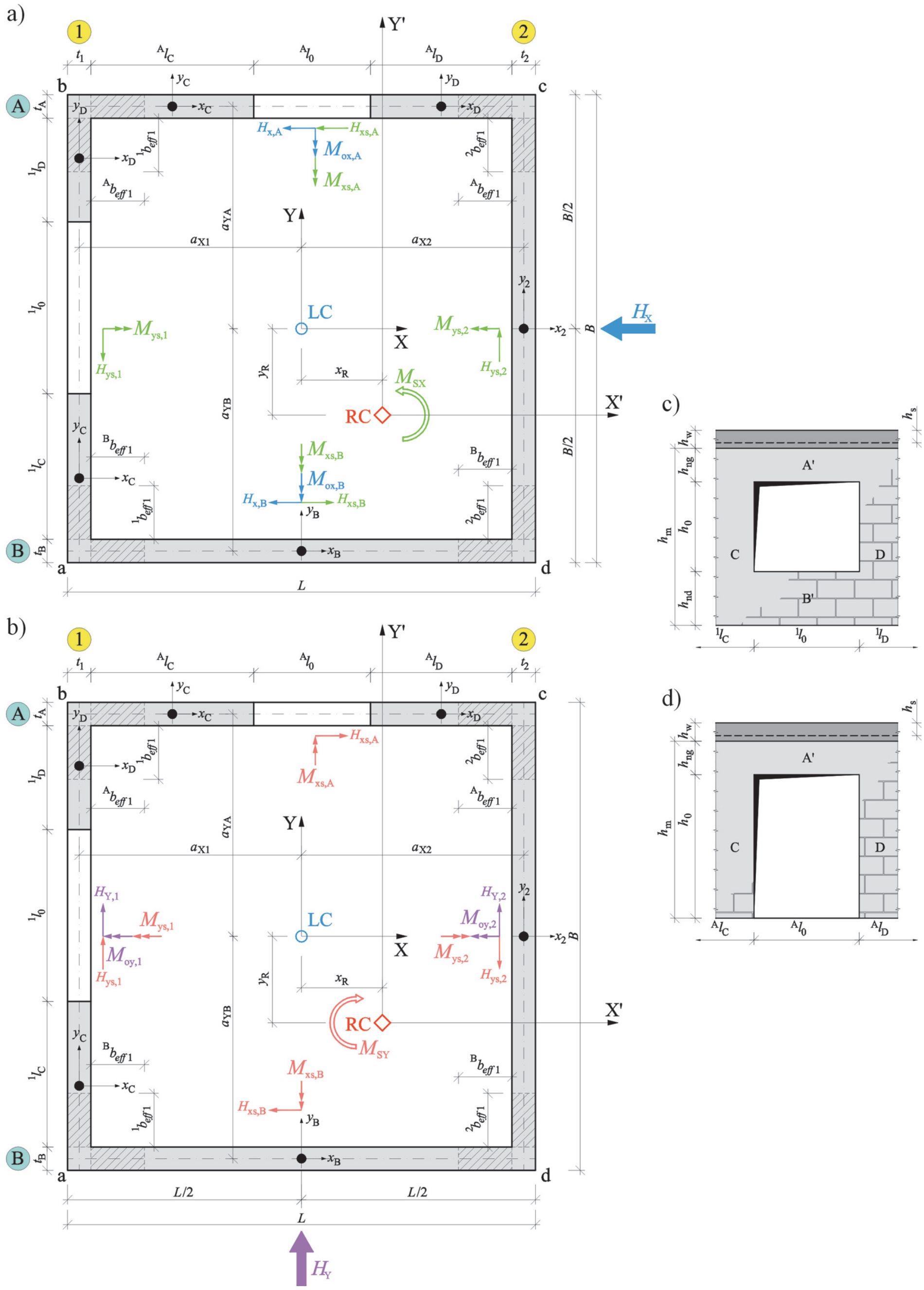

Fig. 3. The geometry of the calculated building: a) internal forces acting on walls under the load of H_X, b) internal forces acting on walls under the load of H_Y, c) a fragment of a wall with a window opening in the axis 1, d) a fragment of a wall with a door opening in the axis A

Table 2. Geometric and stiffness characteristics of models' walls

A wall or a wall component		Moment of inertia I, m^4	Surface area A, m^2	Wall model	Distance between the gravity centre of the wall to the LC point a, m	Wall stiffness K, MN/m	
1	A′	$I_{yA'} = 1.59$ m^4	4.18 m^2	"F"	$a_{x1} = -1.91$ m	$K_{x.A'} = 592.8$ MN/m	$K_{x,1} = 102.4$ MN/m $(K_{x,1} = 96,4$ MN/m$)^*$
	B′	$I_{yA'} = 1.59$ m^4	4.18 m^2	"F"		$K_{x.B'} = 294.9$ MN/m	
	C	$I_{yC} = 0.09$ m^4	0.09 m^2	"F" ("C")		$K_{x.C} = 106.6$ MN/m $(K_{x.C} = 94.4$ MN/m$)$	
	D	$I_{yC} = 0.09$ m^4	0.09 m^2	"F" ("C")		$K_{x.D} = 106.6$ MN/m $(K_{x.C} = 94.4$ MN/m$)$	
2		$I_{x2} = 1.59$ m^4	4.18 m^2	"F"	$a_{x2} = 1.91$ m	$K_{x.2} = 114.0$ MN/m	
A	A′	$I_{yA'} = 1.59$ m^4	4.18 m^2	"F"	$a_{xA} = 1.91$ m	$K_{y.A'} = 592.8$ MN/m	$K_{y,A} = 81.5$ MN/m $(K_{y,A} = 58.5$ MN/m$)^*$
	C	$I_{yC} = 0.09$ m^4	0.09 m^2	"F" ("C")		$K_{y.C} = 47.2$ MN/m $(K_{y.C} = 32.4$ MN/m$)$	
	D	$I_{yD} = 0.09$ m^4	0.09 m^2	"F" ("C")		$K_{y.D} = 47.2$ MN/m $(K_{y.C} = 32.4$ MN/m$)$	
B		$I_{yB} = 1.59$ m^4	4.18 m^2	"F"	$a_{xB} = -1.91$ m	$K_{y.B} = 114.0$ MN/m	

Remark!
Stiffnesses determined in the cantilever static schemes of inter-hole pillars are given in brackets.
* – wall stiffness calculated with cantilever stiffness of inter-hole pillars.

Table 3. Results of internal forces in the building walls based on the analytical model

Load variant	Wall	$H_{x,i}$ kN	$H_{xs,i}$ kN	$H_{y,i}$ kN	$H_{ys,i}$ kN	$H_x = H_{x,i}+H_{xs,i}$ kN	$H_y = H_{y,i}+H_{ys,i}$ kN	$M_{ox,i}$ kNm	$M_{oy,i}$ kNm	$M_{sx,i}$ kNm	$M_{sy,i}$ kNm	$M_x = M_{ox,i}+M_{sx,i}$ kNm	$M_y = M_{oy,i}+M_{sy,i}$ kNm
$H_x = -1$ kN	1	–	–	–	–0.04 (–0.09)	–	–0.04 (–0.09)	–	–	–	0.11 (0.23)	–	0.11 (0.23)
	2	–	–	–	0.04 (0.09)	–	0.04 (0.09)	–	–	–	–0.11 (–0.23)	–	–0.11 (–0.23)
	A	–0.42 (–0.34)	–0.04 (–0.07)	–	–	–0.46 (–0.41)	–	–1.05 (–0.85)	–	–0.10 (–0.17)	–	–1.15 (–1.02)	–
	B	–0.58 (–0.66)	0.04 (0.07)	–	–	–0.54 (–0.59)	–	–1.46 (–1.66)	–	0.10 (0.17)	–	–1.36 (–1.49)	–
$H_y = -1$ kN	1	–	–	0.47 (0.46)	0.014 (0.024)	–	0.48 (0.48)	–	–1.19 (–1.15)	–	–0.04 (–0.06)	–	–1.23 (–1.21)
	2	–	–	0.53 (0.54)	–0.014 (–0.024)	–	0.52 (0.52)	–	–1.32 (–1.36)	–	0.04 (0.06)	–	–1.28 (–1.30)
	A	–	0.013 (0.018)	–	–	0.013 (0.018)	–	–	–	–0.03 (–0.04)	–	–0.03 (–0.04)	–
	B	–	–0.013 (–0.018)	–	–	–0.013 (–0.018)	–	–	–	0.03 (0.04)	–	0.03 (0.04)	–

Remark!
Stiffnesses determined in the cantilever static schemes of inter-hole pillars are given in brackets.

In addition to the analytical solution, numerical FEM models of the analyzed buildings were made. Four-node shell finite elements with six degrees of freedom at each node are used. The model was articulated non-displaceable in each node located on the lower edge of the wall. The finite elements representing the walls and lintels were given the parameters (E_m, ν_m). The reinforced concrete slab and ring beam was assumed the parameters of concrete class C20/25. No degrees of freedom were released in the finite element nodes between walls, slab and ring beam, maintaining the inseparability of displacements and deformations. The numerical FEM model is shown in Fig. 4.

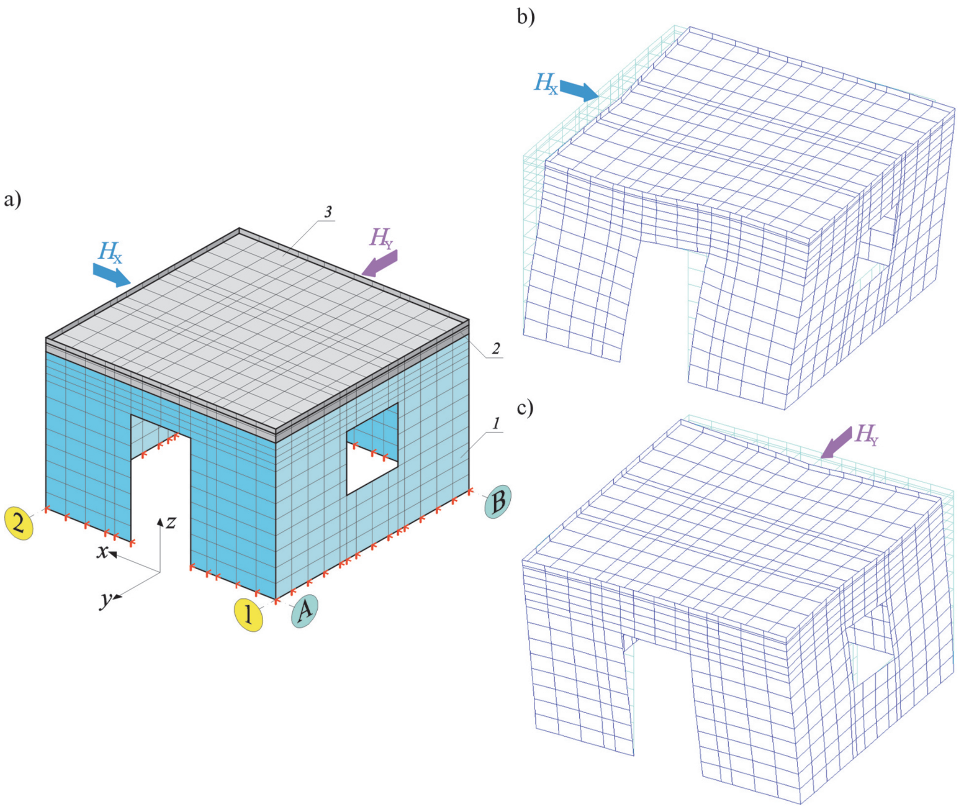

Fig. 4. Numerical FEM model of the building a) 3D view of the model with loads in variant I – force $H_X = -1$ kN and in variant II – force $H_y = -1$ kN b) model displacements as a result of the H_x force (variant I) c) model displacements as a result of the H_y force (variant II); 1 – masonry made of AAC, 2 – ring beam, 3 – floor slab

The calculation of the shear forces in walls in each load variant made it possible to determine the location of the stiffening centre of the FEM model. A static method was used, formulating equations of bending moments in relation to the RC point in both load variants and determining the coordinates of the stiffening centre by the (5.1) and (5.2) dependencies. The analytical and FEM results were compared in Table 4.

Table 4. Results of internal forces in the building walls based on the FEM model

Load variant	Wall	$MES\,H_x = (H_{x,i} + H_{xs,i})$ kN	$MES\,H_y = (H_{y,i} + H_{ys,i})$ kN	$MES\,M_x = (M_{ox,i} + M_{sx,i})$ kNm	$MES\,M_y = (M_{oy,i} + M_{sy,i})$ kNm	$\frac{H_x}{MES\,H_x}$	$\frac{H_y}{MES\,H_y}$	$\frac{M_x}{MES\,M_x}$	$\frac{M_y}{MES\,M_y}$
$H_x = -1$ kN	1	–	–0.07	–	0.16	–	0.61 (1.28)	–	0.69 (1.45)
	2	–	0.07	–	–0.16	–	0.61 (1.28)	–	0.69 (1.45)
	A	–0.43	–	–0.93	–	**1.07 (0.95)**	–	**1.23 (1.10)**	–
	B	–0.57	–	–1.61	–	**0.95 (1.03)**	–	**0.85 (0.92)**	–
$H_y = -1$ kN	1	–	0.46	–	–1.06	–	**1.04 (1.04)**	–	**1.16 (1.14)**
	2	–	0.54	–	–1.48	–	**0.96 (0.96)**	–	**0.86 (0.88)**
	A	0.04	–	–0.13	–	0.32 (0.44)	–	0.23 (0.31)	–
	B	–0.04	–	0.13	–	0.32 (0.44)	–	0.23 (0.31)	–

Remark!
Stiffnesses determined in the cantilever static schemes of inter-hole pillars are given in brackets.

$$ {}^{MES}x_R = \frac{0.5L({}^{MES}H_{y,1} - {}^{MES}H_{y,2}) + 0.5B({}^{MES}H_{x,A} - {}^{MES}H_{x,B})}{H_y + {}^{MES}H_{y,1} + {}^{MES}H_{y,2}} = 0.08 \text{ m} \tag{5.1} $$

$$ {}^{MES}y_R = \frac{0.5B({}^{MES}H_{x,B} - {}^{MES}H_{x,A}) + 0.5L({}^{MES}H_{y,1} - {}^{MES}H_{y,2})}{H_x + {}^{MES}H_{x,A} + {}^{MES}H_{x,B}} = -0.32 \text{ m} \tag{5.2} $$

6. Discussion

The coordinates of the rotation centre determined by the analytical method with the pillars fixed on both sides were $x_R = 0.10$ m and $y_R = -0.32$ m, and by cantilever static scheme of pillars, the coordinates of the RC point were $x_R = 0.16$ m and $y_R = -0.61$ m. For the double-fixed static scheme, the distances to the LC point accounted for 3% and 8% of the wall length. In the cantilever model, the analyzed values accounted for 4% and 16% of wall length. According to the national guidelines [6], the coordinates were > 5% the wall's length, and it was required to take into account the influence of torsion. In the FEM model, the coordinates of the rotation centre were (${}^{MES}x_R = 0.08$ m; ${}^{MES}y_R = -0.32$ m) and almost coincided with the analytical model in which inter-hole pillars were fixed on both sides. The shear forces acting on walls, calculated by Eurocode 6 [1], with different static schemes of inter-hole pillars, were compared with the FEM numerical model. The calculations with inter-hole pillars fixed on both sides were analyzed. In case I – in the unloaded walls 1 and 2 parallel to the Y-axis, about 39% underestimating the shear forces was obtained. In the A and B loaded walls parallel to the X-axis, the forces calculated according to the FEM model did not differ significantly from the analytically determined forces (in the A and B wall, the calculated force was 7% higher, and in the B wall 5% lower than the FEM results). Similar results were for the bending moments in walls 1 and 2. The total bending moments were over 31% underestimated. The most negligible difference of total bending moments was in the loaded walls. Over 23% overestimation of bending moments was obtained in the analytical method for wall A. In the B-axis wall, the analytical method enabled the determination of the bending moment with over 15% underestimation. In a building loaded with H_Y force, over 68% underestimation of shear forces was obtained in the A and B walls perpendicular to the load direction (parallel to the X-axis). A much greater convergence was obtained in walls 1 and 2 located parallel to the direction of the load. The force in wall 1, calculated according to the analytical model, was 4% higher, and in wall 2 – 4% lower than the forces determined with FEM. Similar results were obtained for bending moments. Compared FEM results, the moment values in walls 1 and 2 were overestimated by 16% for wall 1 or underestimated by 24% for wall 2. The most remarkable differences were found in the walls perpendicular to the load direction – in the A and B walls – the underestimation of bending moments was over 77%. Assuming the cantilever scheme of inter-hole pillars and the load of the model with the H_X force in the unloaded walls 1 and 2 (parallel to the Y-axis) – over 28% overestimating the shear forces were obtained. In the A and B walls located in the load's direction, the forces calculated by the FEM model did not differ by more than 5% compared to analytical calculations. The bending moments in the unloaded walls 1 and 2 were over 45% higher than the FEM results. The noticeable convergence of bending moments was obtained in the loaded walls A and B. In the wall with the door opening, a 10% overestimation of bending moments was obtained. In the wall with a window opening, the underestimation was 8%, according to the analytical method. With the load acting parallel to the Y-axis in the walls located perpendicular to the load direction (A and B), over 56% underestimating the shear forces was obtained. A greater convergence was obtained in the walls located parallel to the direction of the load (1 and 2). The difference between the analytical and the FEM model did not exceed 4%. Similar results were obtained for bending moments. The most significant underestimation of the results was in A and B walls, where the difference to the FEM calculations was over 69%. In walls 1 and 2 parallel to the acting load, the moment values were overestimated by 14% in wall 1 or underestimated by 12% in wall 2 (compared to the FEM method).

The convergence of rotation centre (RC) in the analytical double-fixed model with pillars compared to the FEM model caused the values of shear forces in the direction of the load did not differ by more than 7%. Nevertheless, the bending moments in these walls differed significantly – even by up to 24%. The differences were significant in the unloaded walls in which the force values depended solely on the stiffening centre. The maximum differences in shear forces were over 68%, and bending moments differed by over 77%.

On the other hand, in the model in which the inter-hole pillars had a cantilevered static scheme, the coordinates of the RC (the rotation centre) point differed significantly compared to the FEM results. Similar results were obtained for the shear forces in the walls in the direction of the load. Compared to the model with fixed inter-hole pillars, the differences in shear forces decreased in walls located perpendicular to the load direction. The situation was analogical in bending moments. The results were similar to those of FEM in the walls located parallel to the load direction. In the walls located perpendicular to concentrated forces, an increase in the value of moments was observed compared to the analytical model.

The analyzes of both static schemes of the inter-hole pillars showed that the changes in the wall stiffness did not have such a significant impact on the values of internal forces in the walls located parallel to the load direction. Greater convergence of internal forces in the direction of load action occurred when changed the static scheme. The static cantilever scheme caused the change of stiffness and the rotation centre (RC) position.

7. Conclusion

An analytical model for calculating internal forces in stiffening walls was proposed, developed following guidelines [21] and taking into account the recommendations of the draft Eurocode 6 [1]. Standard recommendations for determining wall geometry and length of perpendicular walls to the stiffening walls were considered (the problem of flanged walls).

It was proposed stiffness of walls without openings using different static schemes, including shear deformations [26–28]. The division method into components was proposed [21, 32] to calculate the masonry's stiffness with openings. The stiffness was determined based on the total displacement of the wall, assuming the model of pillars with double-fixed sides or with a cantilever model. Wall stiffness was used to calculate the rotation centre and to distribute shear forces and bending moments in the walls. An example of a building with an uncomplicated wall layout was used to verify the proposed method.

Two walls had a door opening or a window opening, and two walls were devoid of perforation. Two variants of loading the force parallel to the longitudinal or transverse axis of the building were considered. The mechanical parameters of the wall made of autoclaved aerated concrete masonry units were adopted from our research [29–31]. Apart from the analytical model, a numerical FEM spatial model was also performed, which was solved in the linear-elastic range. A high convergence of the rotation centre location (RC) was demonstrated in both models with the assumpted double-fixed static scheme. When the pillars represented as cantilever bars, the position of the RC point was significantly different from the coordinates determined by the FEM method.

Although the stiffening centre in the analytical model (with double-fixed pillars) and the FEM model were very similar, significant differences in internal forces were obtained in each calculation variant. In transverse forces in the walls parallel to the direction of the load, the difference in forces did not exceed 7%. In contrast, in the walls perpendicular to the load direction, the force values were underestimated even by 68%. A similar situation occurred in the estimation of bending moments. In walls in the direction of load – bending moments did not differ by more than 23%, while in walls perpendicular to the direction of load, the difference even exceeded 77%. Different values of coordinates the position of the RC point were obtained in cantilever static wall models. The differences in internal forces in the walls located in the load direction compared to the double-fixed model have noticeable decreased. In walls located perpendicular to the load direction, the differences in the values of internal forces compared to the FEM model were significantly reduced. The convergence of the rotation centre position (RC) in the double-fixed model may indicate that the walls' stiffness influenced results. Calculations bases on the cantilever scheme showed a change in the position of the RC point. In turn, this did not cause an evident change of internal forces in the walls in the direction of the load but caused a noticeable change of forces in the other walls.

To sum up, the proposed method enables calculation of buildings with a simple wall layout with openings for:

a) safe estimation of internal forces in walls located in the direction of load action, regardless of the applied static scheme of the pillars,
b) underestimating internal forces in walls located perpendicular to the direction of the load in both static schemes of pillars.

The proposed method requires analyses aimed at:

a) validation of the length of perpendicular walls connected with stiffening walls,
b) development of a methodology for various ways of connecting walls,
c) taking into account various support and load conditions,

d) considering changes in wall stiffness caused by scratches,
e) safe wall displacement calculation to control Serviceability Limit State (SLS) conditions.

As part of the verification of the proposed method, experimental tests of the building model, presented in the calculation example, are carried out at the Silesian University of Technology.

References

[1] EN-1996-1-1:2019 Eurocode 6. Design of masonry structures. Part 1-1: General rules for reinforced and unreinforced masonry structures.

[2] A.W. Hendry, B.P. Sinha, S.R. Davies, *Design of Masonry Structures*. Third ed. London: E&FN SPON, 2004.

[3] PN-B-03002:1954 Konstrukcje murowe z cegły. Obliczenia statyczne i projektowanie.

[4] PN-B-03002:1967 Konstrukcje murowe z cegły. Obliczenia statyczne i projektowanie.

[5] PN-B-03002:2007 Konstrukcje murowe. Projektowanie i obliczanie.

[6] B. Lewicki, J. Bielawski, J. Sieczkowski, *Budynki murowane. Zasady Projektowania z przykładami obliczeń*. Warszawa: Centralny Ośrodek Badawczo-Projektowy Budownictwa Ogólnego. 1993.

[7] DIN 1053-1 Mauerwerk. Teil 1: *Rezeptmauerwerk. Berechnung und Ausfurung/Ausgabe. 1990*.

[8] *International Recommendations for Masonry Structures*. CIB W23. CIB Report, Publication 58/1980.

[9] A. Cholewicki, *Obliczanie ścian usztywniających*. Warszawa: Centralny Ośrodek Badawczo-Rozwojowy Budownictwa Ogólnego, 1980.

[10] PN-B-03002:1999/Az1+Az2: Konstrukcje murowe niezbrojone. Projektowanie i obliczanie.

[11] ENV-1996-1-1:2002-Eurocode 6: Design of Masonry Structures. Part 1-1:Common Rules for Reinforced and Unreinforced Masonry Structures. CEN / TC 250, march 2003.

[12] PN-EN 1996-1-1:2010/AC 2009 Eurokod 6. Projektowanie konstrukcji murowych – Cześć 1-1: Reguły ogólne dla zbrojonych i niezbrojonych konstrukcji murowych.

[13] BS 5628-1:1992 Use of Masonry – Part 1: Structural use of unreinforced masonry. BSI 1992.

[14] I.S. 325 Part 1:1986 Code of practice for use of masonry. Part 1: Structural use of unreinforced masonry. National Standards Authority of Ireland. Dublin 1986.

[15] DIN 1053-100:2007-09 Mauerwerk. Teil 100: Berechnung auf der Grundlage des semiprobabilistischen Sicherheitskonzepts. Deutsches Institut für Normung e.V.: Beuth Verlag Berlin 2007.

[16] DIN 1053-1:1996-11 *Mauerwerk. Teil 1: Berechnung und Ausführung*. Deutsches Institut für Normung e.V.: Beuth Verlag Berlin 1996.

[17] SIA 177/2:1992. *Bemessung von Mauerwerkswänden*. SIA, Zürich 1992.

[18] SIA 266:2003 *Masonry*. Swiss Society of Civil Engineers and Architects. Zurich 2003.

[19] NS 3475:1981 *Prosjektering av murverk. Beregnig og dimensjonering*.

[20] SNiP II-22-81:2000. Kamiennyje i armokamiennyje konstrukcji (in Russian).

[21] National Building Code of Canada (NBCC) 2005.

[22] ACI-530-92/ASCE 5-92/TMS 420-92: *Building Code Requirements for Masonry Structures*. Masonry Standards joint Committee. ACI Detroit, ASCE New York, TMS Bulder, 1992.

[23] *Masonry Structural Design for Buildings*. Departments of the Army, the Navy, and the Air Force. ARMY TM 5-809-3, NAVY NAVFAC DM-2.9, AIR FORCE AFM 88-3, Chap. 3, October 1992.

[24] GB 50003-2001:2001 *Code for Design of Masonry Structures*. Beijng, 2002.

[25] W. Jäger, "Unreinforced masonry – shear loadingin E*N 1996 Design of masonry Structures. A dissemination of information for training workshop – Brussels, 2–3 April 2009* (CD-ROM).

[26] K. Zilch, D.C. Schermer, S. Grabowski, W. Scheufler, "Boundary conditions of shear walls in multi-storey masonry structures under horizontal loadings in P*roceedings of* 7^{th} *International Brick/Block Masonry Conference, Sydney 2008* (CD-ROM).

[27] K. Grikmamn, *Flächentragwerke – Einführung in die Elastostatik der Scheiben, Platten, Schalen und Faltwerke*. Vienna: Springer, 1958, DOI: 10.1007/978-3-7091-4386-5.

[28] S. Timoshenko, J.N. Goodier, *Theory of Elasticity*. New York, Toronto, London: McGraw-Hill Book Company, Inc., 1951.

[29] R. Jasiński, "Effects of Opening Shapes on Behaviour of Shear Walls Made of AAC Masonry Units *IOP Conference Series: Materials Science and Engineering,* 2019, vol. 471, DOI: 10.1088/1757-899X/471/2/022011.

[30] R. Jasiński, "Research and modeling of masonry shear walls". PhD DsC Thesis. Silesian University of Technology, Gliwice, Poland 2017. ISBN 978-83-7880-477-2 (In Polish).

[31] R. Jasiński, Ł. Drobiec, "Effects of Technology of Placing Different Types of Reinforcement in Bed Joints on Compressive and Shear Strength of AAC Masonry Walls *IOP Conference Series: Materials Science and Engineering,* 2019, vol. 471, DOI: 10.1088/1757-899X/471/2/022010.

[32] *Masonry Structural Design for Buildings*. Departments of the Army, the Navy, and the Air Force. ARMY TM 5-809-3, NAVY NAVFAC DM-2.9, AIR FORCE AFM 88-3, Chap. 3, October 1992.

Adaptacja metody całkowitej sztywności do rozdziału obciążeń na murowe ściany usztywniające według Eurokodu 6

Słowa kluczowe: konstrukcje murowe, ściany usztywniające, rozdziałobciążeń, środek skręcania

Streszczenie:

Zasadniczym celem pracy była adaptacja metody całkowitej sztywności ścian do rozdziału obciążeń na ściany usztywniające w budynku o prostym układzie ścianowym według ogólnych zaleceń Eurokodu 6. Na wstępie przedstawiono normowe zalecenia dotyczące ścian usztywniających podane w Eurokodzie 6. Następnie zaproponowano uszczegółowienie procedury obliczeniowej. Przyjętą procedurę porównano z wynikami obliczeń MES modelu budynku o prostym układzie ścianowym. Większość zaleceń normowych nie podaje szczegółowych wytycznych i procedur rozdziału siłoraz wyznaczania siłwewnętrznych w murowanych ścianach usztywniających. Przepisy ograniczają się do ogólnych zaleceń dotyczących identyfikacji ścian usztywniających, ewentualnej współpracy z innymi elementami budynku oraz do opisu warunków konstrukcyjnych. Dotyczy to również projektu Eurokodu, 6 w którym jednak do stosowania dopuszczono wiarygodne metody analityczne lub metody numeryczne bazujące na MES. W pracy dokonano adaptacji przepisów kanadyjskich (National Building Code of Canada (NBCC) 2005) do opracowania metody obliczania całkowitej sztywności ściany. Uwzględniając zapisy Eurokodu 6 (w aspekcie współpracy z innymi ścianami) wyznaczono zależności pozwalające na wyznaczenie przemieszczeń ściany z otworami, dzięki podziałowi na elementy składowe. Przemieszczenia składowych elementów ściany wyznaczono w zależności od geometrii i warunków brzegowych ściany. Przy obliczeniach całkowitej sztywności ściany uwzględniono odkształcenia giętne oraz postaciowe.

Następnie podano zależności pozwalające wyznaczyć położenie środka skręcania budynku RC. Oprócz tego podano kompletne podejście umożliwiające rozdział sił wewnętrznych na poszczególne ściany. Zaproponowaną metodę zweryfikowano obliczeniowo posługując się przykładem budynku o nieskomplikowanym kształcie wykonanym z elementów murowych z autoklawizowanego betonu komórkowego z żelbetowym stropem i obwodowym wieńcem. W celu uwypuklenia zachodzących zjawisk w ścianach wykształtowano otwór okienny i otwór drzwiowy. Obliczenia wykonano przy

założeniu działania obciążenia w kierunku długości jak i szerokości. Oprócz tego zróżnicowano schematy statyczne filarków międzyotworowych zakładając model pręta obustronnie utwierdzonego oraz model wspornikowy. Do weryfikacji metody analitycznej wykonano także model MES budynku o identycznej geometrii i warunkach początkowo- brzegowych jak w metodzie analitycznej.

Mimo, że współrzędne środka skręcania budynku w modelu analitycznym (z obustronnie utwierdzonymi filarkami) i w modelu MES były bardzo zbliżone to uzyskano zasadnicze różnice sił wewnętrznych w poszczególnych wariantach obliczeń. W przypadku sił poprzecznych w ścianach leżących równolegle do kierunku działania obciążenia różnica sił nie przekroczył a 7%, natomiast w ścianach leżących prostopadle do kierunku działania obciążenia – wartości sił były niedoszacowane nawet o 68%. Podobna sytuacja wystąpiła analizując wartości momentów zginających. W ścianach leżących na kierunku działania obciążenia momenty zginające nie różniły się więcej niż o 23%, natomiast w ścianach prostopadłych do kierunku działania obciążenia różnica przekroczyła nawet 77%. W przypadku, gdy zastosowano wspornikowe modele filarków międzyotworowych uzyskano wyraźnie inne współrzędne położenia punktu RC. W tym przypadku różnice sił wewnętrznych w ścianach położonych na kierunku działania obciążenia w stosunku do modelu z filarkami obustronnie utwierdzonymi istotnie zmalały. Natomiast w ścianach położonych prostopadle do kierunku obciążenia różnice wartości sił wewnętrznych w stosunku do modelu MES uległy znacznemu zmniejszeniu. Zbieżność współrzędnych środka skręcania (RC) w modelu, w którym zastosowano obustronne utwierdzenie filarków międzyotworowych może wskazywać, że czynnikiem wpływającym na uzyskiwane rezultaty była sztywność ścian. Z kolei obliczenia w których zmieniono schemat statyczny filarków na wspornikowy wykazały zmianę położenia punktu RC. To z kolei nie wywołało wyraźnej zmiany sił wewnętrznych w ścianach na kierunku działania obciążenia, ale spowodowało wyraźną zmianę siłw pozostałych ścianach.

Reasumując, zaproponowana metoda umożliwia w budynkach o nieskomplikowanym układzie ścian z otworami na:

a) bezpiecznie zawyżone oszacowanie sił wewnętrznych w ścianach leżących na kierunku działania obciążenia bez względu na zastosowany schemat statyczny filarków,
b) niedoszacowanie sił wewnętrznych w ścianach położonych prostopadle do kierunku działania obciążenia w obydwu schematach statycznych filarków.

Received: 5.05.2021, Revised: 9.07.2021